

Electronic Supplementary Information for

Flexible Conductive Porous Fibrillar Polymer Gold Nanocomposites with Enhanced Electromagnetic Interference Shielding and Mechanical Properties

Jun Li,^a Hu Liu,^b Jiang Guo,^b Zhen Hu,^a Zhijiang Wang,^a

Bin Wang,^c Li Liu,^a Yudong Huang,^{a,*} and Zhanhu Guo^{b,*}

^aSchool of *Chemical* Engineering and Technology,
State Key Laboratory of Urban Water Resource and Environment,
Harbin Institute of Technology, Harbin 150001, China.

^bIntegrated Composites Laboratory (ICL),
Department of Chemical and Biomolecular Engineering,
University of Tennessee, Knoxville, TN USA 37996

^cEngineered Multifunctional Composites (EMC) Nanotech LLC, Knoxville, TN 37934 USA

*To whom correspondence should be addressed.

Email: huangyd@hit.edu.cn (Y. H.) and zguo10@utk.edu (Z. G.)

PIPD macromolecules were synthesized with the established protocols^{1,2} and the long PIPD fibers with a diameter of 45 μm were made with dry-jet wet spinning technology. And then, long PIPD fibers were dispersed in DMSO. A PIPD nanofiber/DMSO solution was obtained after swelling long PIPD fibers in DMSO at 160 °C for 6 h followed by ultrasonication treatment at 90 °C for 2h. At last, the PIPD nanofibers were obtained by centrifugation of the dispersed solution. The distinctive nanostructure of the PIPD nanofibers can be seen in SEM images in **Fig. S1**. Therefore, it can be concluded that the the swell-ultrasonication method is an efficient way for preparing PPIPD nanofiber.

After that, the preparation of the PIPD-based macroinitiator was carried out according to the procedure shown in Scheme 1. In a glass flask, a total of 0.1 g PIPD and 1mL pyridine was dispersed in 300 mL anhydrous chloroform, and the mixture was stirred at 5 °C until the PIPD was dispersed well. And then the flask was cooled to lower than 5 °C by ice water. Then, 2-Bromopropionyl bromide (0.22 g, 10 mmol) in 10.0 mL chloroform was added dropwise into PIPD solution. After the dropping process was completed, the ice water was maintained for another 30 min and then removed. The reaction was stopped after 96 h and the resulting solution was poured into excess amount of ethanol and precipitated as red floccules. The products were washed thoroughly with ethanol, and then dried by freeze-drying, in around 99% yield.

At last, the macroinitiator PIPD-Br was used to initiate the polymerization of DMDAAC via ATRP using CuBr/triethylamine as a catalyst system.^[3-5] In a general procedure, PIPD-Br (45 mg, 0.1 mmol of Br), DMDAAC (3.46 g, 22.0 mmol), triethylamine (22 μL , 0.1 mmol), and

water (50.0 mL) were added into a flask with a magnetic stirring under argon protection. The PIPD-Br macroinitiator was dispersed in DMDAAC aqueous solution for 8 h, and then Cu(I)Br (14 mg, 0.1 mmol) was added and mixed with another 30 min. Thereafter, the flask was immersed into an oil bath at 43 °C for 2 h, and then the temperature was increased to 60 °C. After a prescribed time period, the polymerization was stopped by exposing the mixture to air and diluted with distilled water. The reaction mixture was dialyzed in a dialysis bag (molecular weight cut off: 8000-10000) against distilled water for 96 h. It was refreshed at an interval of 8 h. Finally, the products were dried by freeze-drying, in around 98% yield.

The dissolution of these samples was also studied. **Fig. S1 h), g) and e)** PIPD/DMSO, PIPD-Br/CH₂Cl₂ and PIPD-g-PDDA/H₂O solution, respectively. PIPD-Br nanofibers show hydrophobic property and look like oil when it was added into water. After grafting of PDDA chains, PIPD fiber can be distributed in water well. PIPD-g-PDDA5 aqueous solution can be kept without deposition for 12 h.

PIP-g-PDDA Porous film was made by filter of PIP-g-PDDA aqueous dispersion (0.1 wt%). And then concentrated aqueous solution of gold NPs was pored through the porous film repeatedly. After a prescribed time, gold NPs were coated onto the surface of PIPD nanofiber by ionic assembly.^[6-9] Obviously, the uniform gold layer^[6-9] was formed on the surface of PIPD nanofiber, as shown in **Fig. S3 b)**. Therefore, the ionic assembly technology can be used to produce connective gold layer. Moreover, the thickness and connectivity of the connective gold layer can be modified by changing the assembling time.

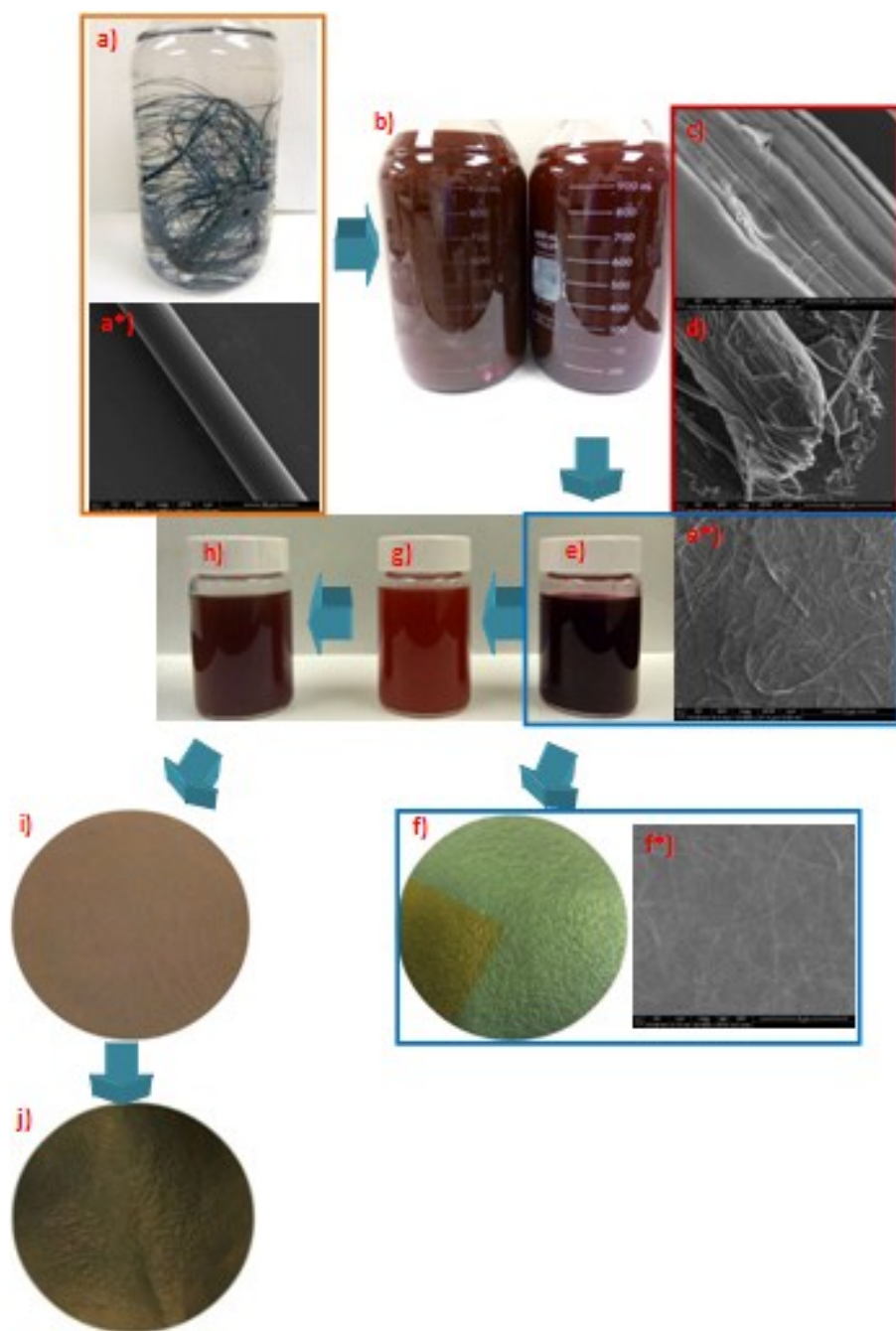


Fig. S1 The morphology of obtained samples during the PIPD-g-PDDA/Au preparation. a) and a*) photo and SEM images of initial PIPD fibers, respectively. b) PIPD nanofiber/DMSO solution. c) and d) the morphology change of the surface of PIPD fiber under strong supersonic oscillation and shearing. It can be seen that PIPD nanofibers were stripped from the initial PIPD fibers gradually. e) PIPD nanofibers dispersed in DMSO. e*) SEM image of the PIPD nanofibers used in the following grafting reaction. f) PIPD film made by using filtration of PIPD/DMSO solution. f*) SEM of PIPD film. g) PIPD-Br nanofibers dispersed in CH_2Cl_2 . h) the PIPD-g-PDDA nanofibers dispersed in H_2O . i) the photography of PIPD-g-PDDA film made by using filtration of PIPD-g-PDDA/ H_2O solution. j) the photography of PIPD-g-PDDA/Au film prepared by using ionic self-assembly.

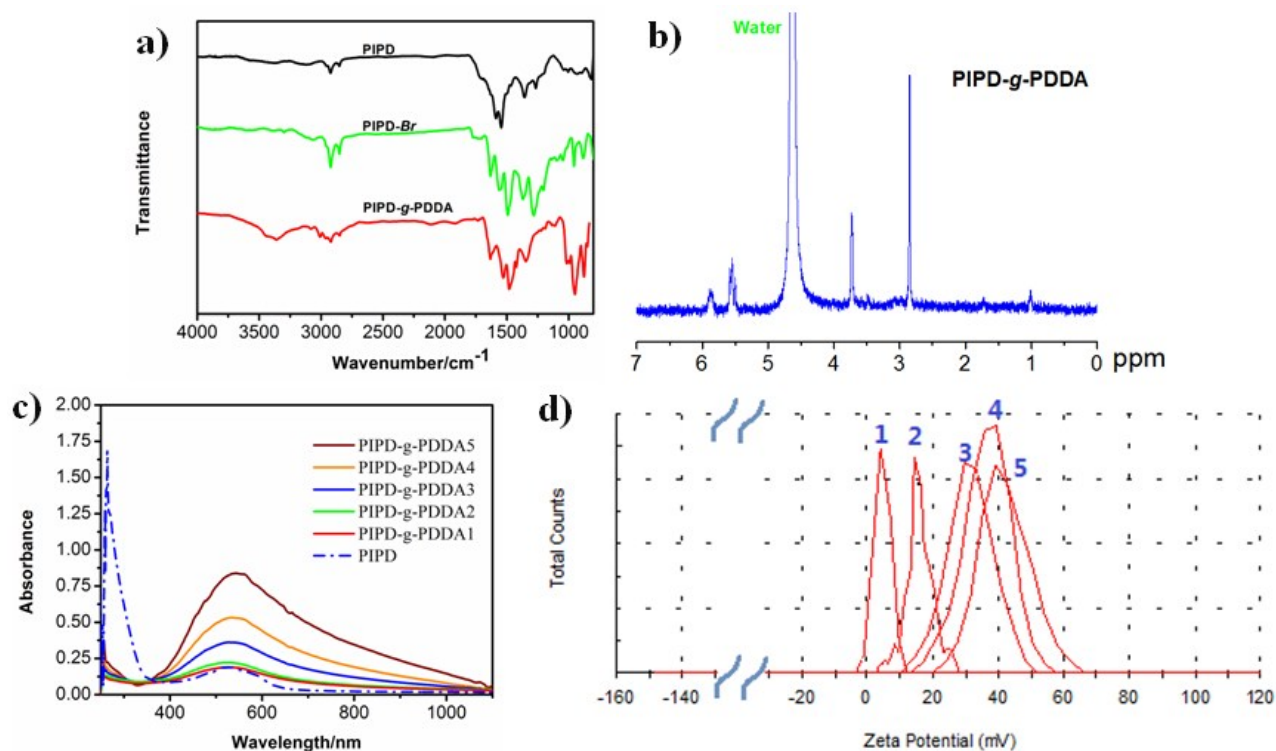


Fig. S2 a) FT-IR spectra of PIPD, PIPD-Br and PIPD-g-PDDA. b) ¹H-NMR spectra of PIPD-g-PDDA5 in deuterium oxide. (c and d) UV and Zeta potential curves of PIPD-g-PDDA with different grafting rate, respectively.

The chemical structures of the samples were characterized in details. **Fig. S2 a)** displays the FT-IR spectra for the virgin PIPD nanofibers, PIPD-Br and PIPD-g-PDDA. The stretching vibration of carbonyl in 2-bromopropionyl group appeared at 1765 cm⁻¹ in the FT-IR spectrum of PIPD-Br, but not in that of its precursor, indicating that the 2-bromopropionyl group was introduced onto PIPD chains.^{10,11} Meanwhile, the characteristic absorption bands of PDDA polymer chain are clearly identified from the spectra of the PIPD-g-PDDA nanofibers. As expected, the water of hydration with PDDA manifests a strong O-H stretching peak at ~3360 cm⁻¹, the absorption bands at ~1632 and ~1482 cm⁻¹ are attributed to the stretch of terminal C=C

bonds.^{12,13} The PDDA grafted on PIPD chains was further confirmed by ¹H-NMR, the chemical shift in the range of $\delta=1.6$ ppm could be attributed to the methyl protons of bromopropionyl group (**Fig. S2 b**). **Fig. S2 c** demonstrates the ultraviolet spectra of PIPD and PIPD-g-PDDA. It can be seen that the ultraviolet absorbance corresponding to the PDDA¹⁴ increases with the grafting and the wavelength at absorbance peak increases from 527.5 to 544.6 nm, meaning that the degree of grafting degree can be controlled by varying the reaction time.

Next we looked into the charging state of PIPD-g-PDDA nanofibers by measuring zeta potential, the results were shown as **Fig. S2 d**. As expected, the PIPD-g-PDDA nanofibers aqueous solution of 0.015 mg/mL showed positively charged, which made the ionic self-assembly of negatively charged gold NPs on the nanofibers much easier. Meanwhile, it can be seen that the zeta potential increases with increasing the reaction time at the beginning, and then comes to a standstill at $\sim +39$ mV. This means that the grafting of PDDA has reached a maximum value for PIPD-g-PDDA5. To estimate the graft ratio, the samples were weighed before and after the graft polymerization with PDDA. The graft ratio (G, wt %) was calculated according to $G=(W_2-W_1)/W_1\times 100$,¹⁵ where W_1 (g) is the dry weight of the PIPD-Br sample and W_2 (g) is the dry weight of the PIPD-g-PDDA sample.

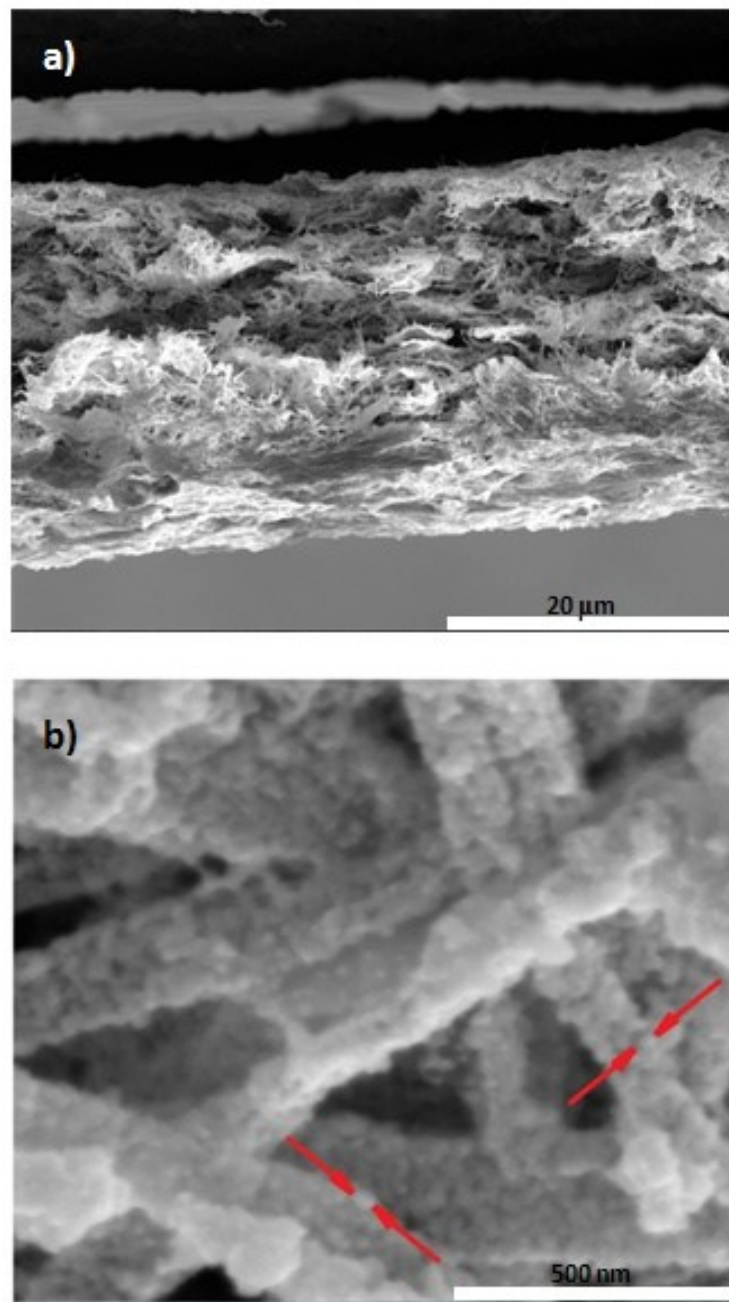


Fig. S3 SEM images of the cross section of PIPD-g-PDDA5 membrane. The thickness of film was read according to the bar.

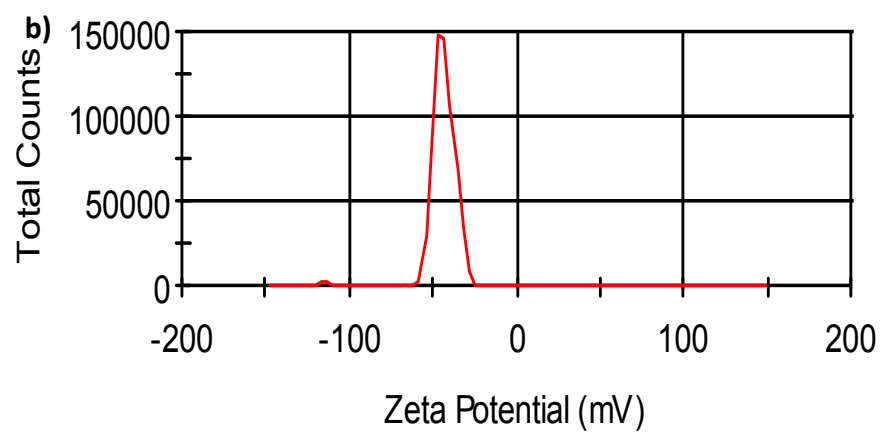
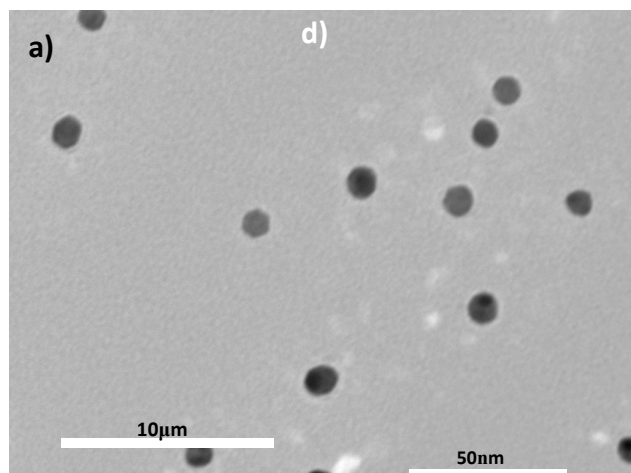


Fig. S4 a) TEM image of gold NPs. b) Zeta potential of gold NPs aqueous solution.

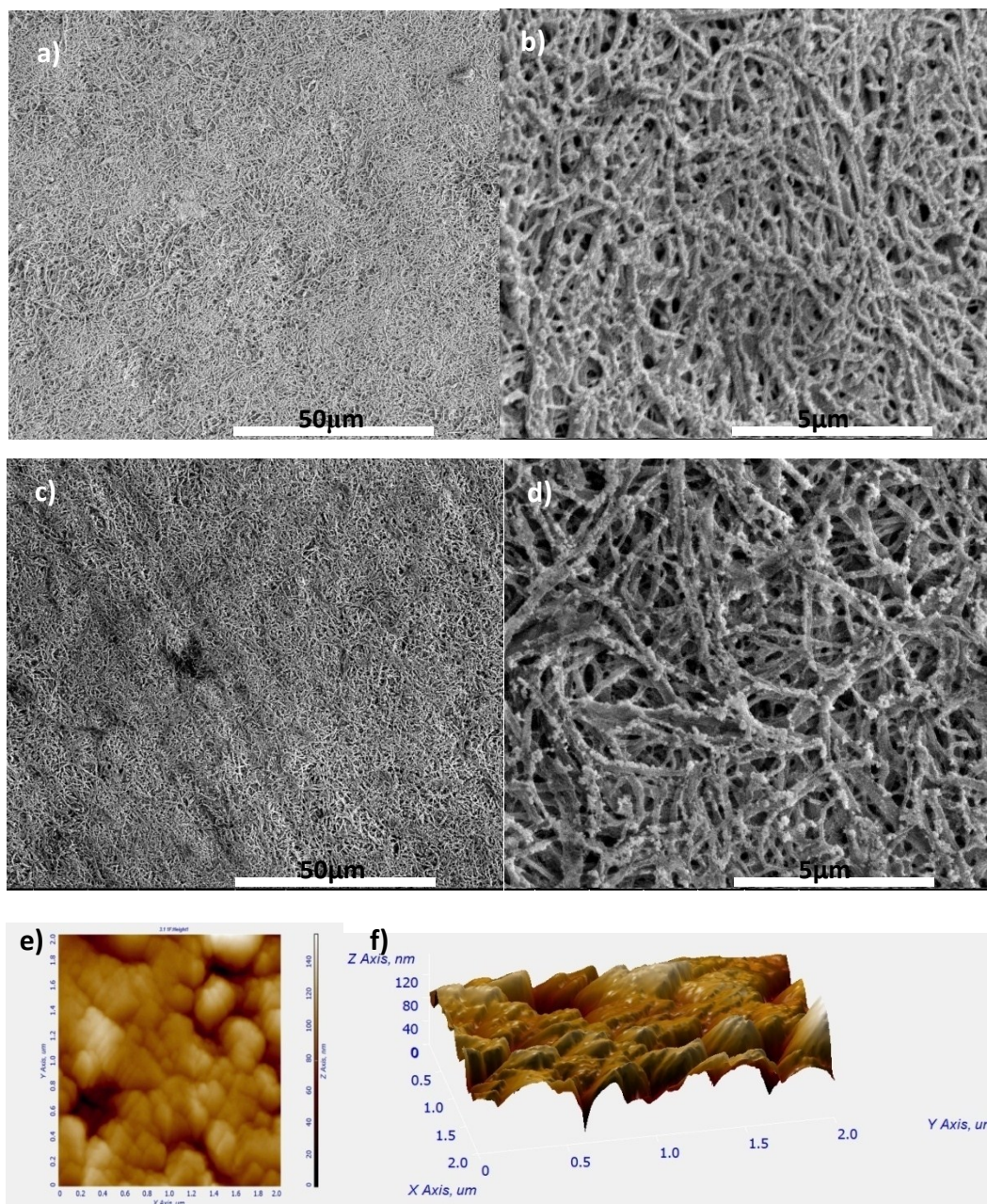


Fig. S5 a) and b) SEM images of PIPD-g-PDDA/Au6 membrane before compression. c) and d) SEM images of PIPD-g-PDDA/Au6 membrane after compression. e) and f) AFM image and corresponding height map of PIPD-g-PDDA/Au6 membrane after compression, respectively.

We speculated that the deformation of gold layer on the PIPD-g-PDDA nanofiber increased with decreasing gold content of the PIPD-g-PDDA/Au composites under the heating treatment. When the content was less than 14.2 v%, the density of the gold NPs is not high enough and the

distance between the neighboring gold NPs will increase when the ligand on the gold NPs evaporated, as shown in **Fig. S6**. Meanwhile, the distance between the neighbor gold NPs of PIPD-g-PDDA/Au composites with gold content higher than 14.2 v% will decrease with heating treatment. Part of the gold particles emerged together and decreased the contact resistance.

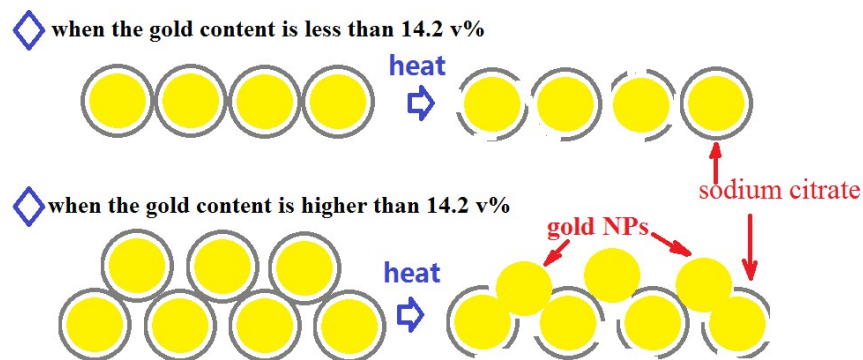


Fig. S6 Scheme of gold layer change on PIPD-g-PDDA/Au composites with different gold content.

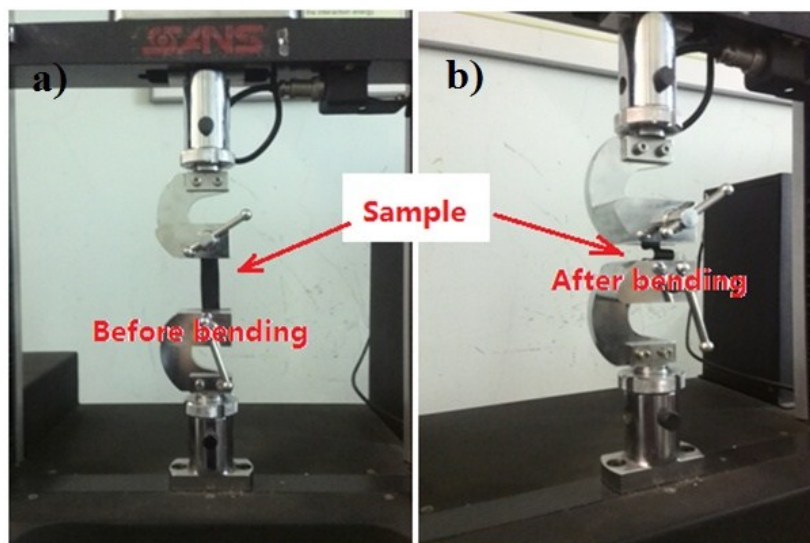


Fig. S7 (a, b) photo of a PIPD-g-PDDA/Au film before and after bending during bending test, respectively.

Due to the excellent flexibility of the PIPD-g-PDDA/Au composites, the conductive property was hold after repeatedly bending cycles. And most of the EMI shielding performance was also maintained because of the great conductive network, show as **Fig. S8**.

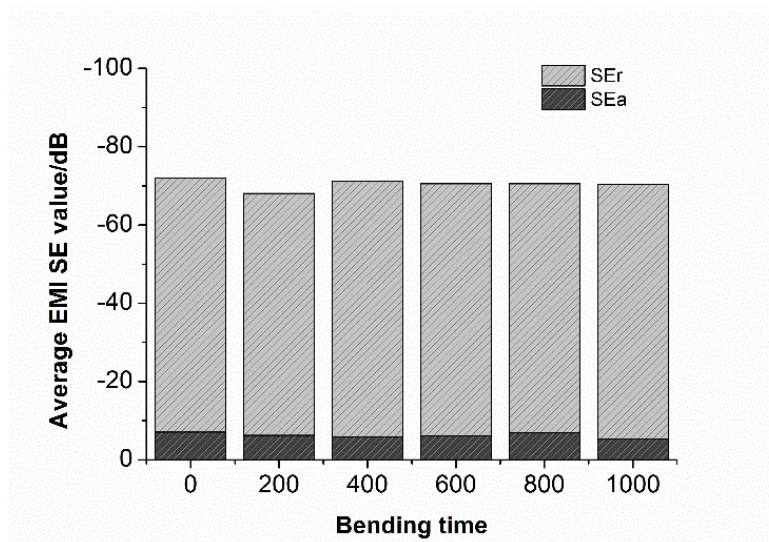


Fig. S8 The change of SE_r and SE_a with bending time.

1. References

1. D. J. Sikkema. *Polymer* 1998, 39, 5981.
2. A. Knijnenberg, J. Bos, T. J. Dingemans. *Polymer* 2010, 51, 1887.
3. S. Ifuku and J. F. Kadla. *Biomacromolecules* 2008, 9, 3308.
4. W. A. Braunecker, K. Matyjaszewski, *Prog. Polym. Sci.* 2007, 32, 93.
5. X. F. Sui, J. Y. Yuan, M. Zhou, J. Zhang, H. J. Yang, W. Z. Yuan, Y. Wei, C. Y. Pan. *Biomacromolecules* 2008, 9, 2615.
6. Y. Y. Yu, Z. G. Chen, S. J. He, B. B. Zhang, X. C. Li, M.C. Yao. *Biosensors and Bioelectronics* 2014, 52, 147.
7. R. Yang, D. D. Miao, Y. M. Liang, L. B. Qu, J. J. Li, Peter de B. Harrington. *Electrochimica Acta* 2015, 173, 839.
8. Z. G. Le, Z. L. Liu, Y. Qian, C. Y. Wang. *Applied Surface Science* 2012, 258, 5348.
9. W. He, H. J. Jiang, Y. Zhou, S. D. Yang, X. Z. Xue, Z. Q. Zou, X. G. Zhang, D. L. Akins, H. Yang. *Carbon* 2012, 50, 265.
10. Y Longiu , V. Klep , B. Zdyrko , I. Luzinov. *Langmuir* 2004, 20(16), 6710.
11. S. Ifuku, John F. Kadla. *Biomacromolecules* 2008, 9, 3308.
12. H. Dautzenberg, E. Gornitz and W. Jaeger, *Macromol. Chem. Phys.*, 1998, 199, 1561.
13. X. X. Zhang, M. L. Chen, Y. L. Yu, T. Yang and J. H. Wang. *Anal. Methods*, 2011, 3, 457.
14. L. F. Hang, C. C. Li, T. Zhang, X. Y. Li, Y. C. Wu, D. D. Men, G. Q. Liu and Y. Li. *RSC Adv.* 2014, 4, 64668.
15. Xiaofeng Sui, Jinying Yuan, Mi Zhou, Jun Zhang, Haijun Yang, Weizhong Yuan, Yen Wei, and Caiyuan Pan. *Biomacromolecules* 2008, 9, 2615.